IEEE Photonics Journal
An IEEE Photonics Society Publication

Open Access

Phase Retrieval of On-Axis Digital Holography With Modified Coherent Diffraction Imaging

Volume 12, Number 6, December 2020

Zhilong Jiang
Xingchen Pan
Xiaoliang He
Yan Kong
Shouyu Wang
Cheng Liu

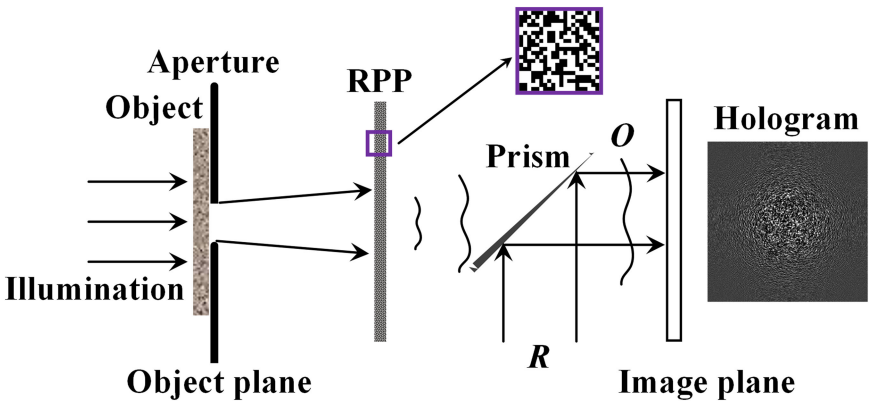

DOI: 10.1109/JPHOT.2020.3035805

Phase Retrieval of On-Axis Digital Holography With Modified Coherent Diffraction Imaging

Zhilong Jiang,[1] **Xingchen Pan**,[2] **Xiaoliang He**,[1] **Yan Kong**,[1] **Shouyu Wang**,[1] **and Cheng Liu**[1,2]

[1]Computational Optics Laboratory, Department of Optoelectric Information Science and Technology, School of Science, Jiangnan University, Wuxi 214122, China
[2]Shanghai Institute of Optics and Fine Mechanics, Chinese Academy of Sciences, Shanghai 201800, China

DOI:10.1109/JPHOT.2020.3035805

Manuscript received September 9, 2020; revised October 24, 2020; accepted October 30, 2020. Date of publication November 4, 2020; date of current version December 4, 2020. This work was supported by the National Natural Science Foundation of China under Grants U1730132, 11947094, 61705092 and the Natural Science Foundation of Jiangsu Province of China under Grants BK20180598, BK20170194. Corresponding authors: Zhilong Jiang; Cheng Liu (email: jiangzl@jiangnan.edu.cn; cheng.liu@hotmail.co.uk.)

Abstract: In this paper, a phase retrieval method is proposed to reconstruct the high-quality image free from undesired terms in on-axis digital holography (DH) with modified coherent diffraction imaging (MCDI). A random phase plate (RPP) is applied to generate a modulated diffraction pattern which forms an on-axis digital hologram with a plane reference wave, and a proper iterative algorithm is designed to reconstruct high-quality object information from both on-axis digital hologram and modulated diffraction pattern. Numerical simulations and experiments prove that both modulus and phase distributions can be accurately reconstructed within 100 iterations while the undesired twin image and zero-order diffraction can be effectively removed, thus demonstrating the feasibility of the suggested method.

Index Terms: Digital holography, image reconstruction.

1. Introduction

As a three-dimensional (3D) imaging technique, digital holography (DH) can record the complete information of an object and reconstruct its quantitative phase and modulus simultaneously. With the advantages of nondestructive, label-free and full field imaging, DH has found many applications in fields of 3D imaging [1], [2], particle tracking [3], [4], bioimaging [5], [6], 3D image recognition and display [7], [8]. However, an inherent drawback of DH is that the undesired twin image and zero-order diffraction are overlapped with the real image. Though off-axis DH [9] can eliminate the undesired information effectively with rather simple operations, it suffers from the resolution reduction due to the limited bandwidth. Therefore, in conditions pursuing high resolution, on-axis DH is still preferred, and on-axis DH reconstruction methods aiming at removing the zero-order diffraction and twin image are still required.

Several techniques [10]–[20] have been applied to remove the undesired terms in on-axis DH. Phase shifting methods [10]–[12] are commonly used to remove the undesired terms and reconstruct the sample image. In these methods, the reference wave phase is varied with a precision

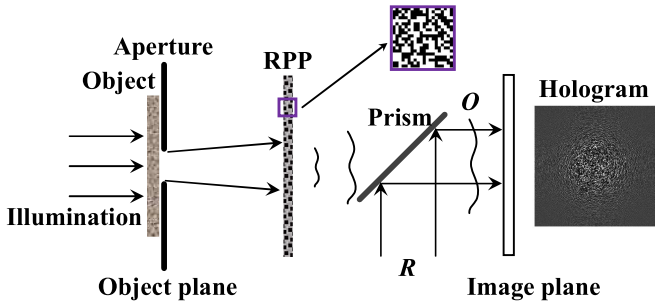

Fig. 1. The schematic of the suggested method.

phase shifting device, and generally more than two phase-shifted on-axis holograms should be captured for object information reconstruction. However, phase shifting methods complicate the experimental implementation due to the requirements on precise phase shifting and multiple hologram recording. Though the parallel phase-shifting DH [13]–[16] and single-shot phase-shifting DH [17], [18] have been proposed, these are at the cost of complexity in system configuration or limited in the field of view (FOV). Besides phase shifting, iterative methods [19]–[22] have also been designed to reconstruct the real image in on-axis DH. Generally no assumption on absorbing or phase shifting of the object is needed and the methods are implemented between object plane and hologram plane with spatial constraints, an algorithm which with forward and backward propagation of the wave-front between these two planes is used to reconstructing modulus and phase distributions of the object quantitatively. While generally a large number of iterations are required before a high quality-image reconstructed with these iteration methods.

To effectively remove the undesired terms and also reduce the number of iterations, we propose a phase retrieval method of on-axis DH with modified coherent diffraction imaging (MCDI). In this method, a dispersed laser beam is used to illuminate the object, a random phase plate (RPP) behind the object is applied to modulate the object information and generate a modulated diffraction pattern, and a CCD camera is adopted to collect the interference between the modulated diffraction pattern and another reference plane wave in on-axis DH mode. A proper iterative algorithm is designed to reconstruct high-quality image from the on-axis digital hologram and the modulated diffraction pattern, and both modulus and phase distributions can be accurately reconstructed within 100 iterations while the undesired twin image and zero-order diffraction can be effectively removed with significantly improved reconstruction quality certificated by both simulations and experiments. It is proved that the proposed method can reconstruct sample information in high quality free from undesired zero-order diffraction and twin image information, moreover, it effectively reduces the iterations and requirements on sensor's dynamic range, therefore, it is a potential tool used in conditions requiring wave-front imaging in high resolution.

2. Principle

The schematic of the suggested method is shown in Fig. 1. An object constrained by an aperture is illuminated with a dispersed laser beam, and then the transmitted light is scattered by an RPP forming a modulated diffraction pattern O on the image plane. This modulated diffraction pattern O next interferes with a plane reference wave R and finally forms an on-axis hologram with the intensity I as

$$I = |O|^2 + |R|^2 + O^* R + O R^* \tag{1}$$

As mentioned in our previous work [23], an RPP can be regarded as a collection of gratings with different periods and directions, thus more diffraction information including high-frequency components of the object can be scattered into the image plane. Moreover, the recorded image become

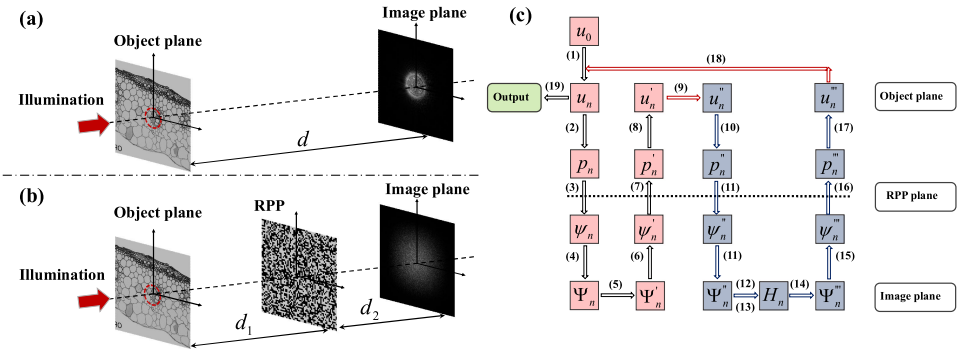

Fig. 2. The diffraction pattern modulated (a) without and (b) with an RPP. (c) Flow chart of the suggested iteration procedure.

uniform since more high-frequency components can be collected by the RPP, which effectively reduces the requirement on sensor's dynamic range. To better understand this, Fig. 2(a) and Fig. 2(b) show the diffraction patterns modulated without and with the RPP, respectively: only a small portion of object information can be collected in Fig. 2(a), while more object information is scattered uniformly into image plane. Therefore, the proposed method should obtain high-quality image reconstruction. Here, an iterative algorithm is designed for sample wave-front retrieval from the on-axis digital hologram and the modulated diffraction pattern, and its flow chart is shown in Fig. 2(c).

1) Give a random guess to the exiting wave of object $u_0(x, y)$ and it serves as the initial guess in the following iterative computation.
2) In the nth iteration, the exiting wave $u_n(x, y)$ is propagated to the RPP plane via Fresnel diffraction to obtain a complex distribution $p_n(x, y)$ shown in Eq. (2), where $\Im_d\{\}$ represents the Fresnel propagation and d_1 is the distance between the object plane and the RPP plane.

$$p_n(x, y) = \Im_{d_1}\{u_n(x, y)\} \tag{2}$$

3) Compute the transmitted field $\psi_n(x, y)$ with Eq. (3) by multiplying $p_n(x, y)$ with the pre-measured RPP transmission function $t(x, y)$.

$$\psi_n(x, y) = p_n(x, y) \cdot t(x, y) \tag{3}$$

4) Propagate the transmitted field $\psi_n(x, y)$ to the image plane to obtain a complex diffraction pattern $\Psi_n(x, y)$ as shown in Eq. (4), in which, d_2 is the distance between the RPP plane and the imaging plane of the CCD camera.

$$\Psi_n(x, y) = \Im_{d_2}\{\psi_n(x, y)\} \tag{4}$$

5) Update $\Psi_n(x, y)$ by replacing the modulus of the diffraction pattern with the square root of the recorded diffraction pattern $I_d(x, y)$ as shown in Eq. (5) and keep phase value unchanged.

$$\Psi'_n(x, y) = \sqrt{I_d(x, y)}\Psi_n(x, y) / \left|\Psi_n(x, y)\right| \tag{5}$$

6) Back propagate $\Psi'_n(x, y)$ to the RPP plane via inverse Fresnel propagation to obtain the updated transmitted field $\psi'_n(x, y)$ as shown in Eq. (5), where $\Im_d^{-1}\{\}$ represents the inverse Fresnel propagation.

$$\psi'_n(x, y) = \Im_{d_2}^{-1}\{\Psi'_n(x, y)\} \tag{6}$$

7) Update the complex distribution before the RPP as $p'_n(x, y)$ using Eq. (7), which is similar to the Wigner-filter and applied to remove the RPP modulation. In addition, β in this equation is a constant used to prevent divide-by-zero effect if $|t(x, y)| = 0$.

$$p'_n(x, y) = p_n(x, y) + \frac{\left|t(x, y)\right|}{\left|t(x, y)\right|_{\max}} \frac{t(x, y)^*}{\left(\left|t(x, y)\right|^2 + \beta\right)} \cdot [\psi'_n(x, y) - \psi_n(x, y)] \tag{7}$$

8) Back propagate $p'_n(x, y)$ to the object plane and obtain the updated exiting wave of the object $u'_n(x, y)$ as shown in Eq. (8).

$$u'_n(x, y) = \Im_{d_1}^{-1}\{p'_n(x, y)\} \tag{8}$$

9) Apply the spatial constraint on the object plane, the exiting wave of the object can be updated as Eq. (9), in which, $u''_n(x, y)$ is the updated exiting wave of object constrained by aperture. $S(x, y)$ used as the spatial constraint has the value of 1 inside the aperture and the value of 0 outside.

$$u''_n(x, y) = [u'_n(x, y) + u_n(x, y)]/2 \cdot \mathrm{S(x, y)} \tag{9}$$

10) Propagate the updated exiting wave of object $u''_n(x, y)$ to the RPP plane to obtain a complex distribution $p''_n(x, y)$ as $p''_n(x, y) = \Im_{d_1}\{u''_n(x, y)\}$.
11) Compute the transmitted field $\psi''_n(x, y)$ as $\psi''_n(x, y) = p''_n(x, y) \cdot t(x, y)$, and then propagate it to the image plane to obtain a complex diffraction pattern $\Psi''_n(x, y)$ as $\Psi''_n(x, y) = \Im_{d_2}\{\psi''_n(x, y)\}$.
12) Compute the complex hologram pattern $H_n(x, y)$ at the image plane from the complex diffraction pattern $\Psi''_n(x, y)$ and the premeasured distribution of reference wave $r(x, y)$ according to Eq. (10).

$$H_n(x, y) = \Psi''_n(x, y) + r(x, y) \tag{10}$$

13) Update $H_n(x, y)$ using Eq. (11) by replacing the modulus of the hologram pattern with the square root of the recorded hologram intensity $I_H(x, y)$ and keep phase value unchanged.

$$H_n(x, y) = \sqrt{I_H(x, y)} H_n(x, y) / \left|H_n(x, y)\right| \tag{11}$$

14) Remove the reference wave $r(x, y)$ to obtain an updated complex diffraction pattern $\Psi'''_n(x, y)$ at the image plane following Eq. (12).

$$\Psi'''_n(x, y) = H_n(x, y) - r(x, y) \tag{12}$$

15) Back propagate $\Psi'''_n(x, y)$ to the RPP plane via inverse Fresnel propagation to obtain the updated transmitted field $\psi'''_n(x, y)$ as $\psi'''_n(x, y) = \Im_{d_2}^{-1}\{\Psi'''_n(x, y)\}$.
16) Update the complex distribution $p'''_n(x, y)$ before the RPP using Eq. (13) to remove the modulation of light beam caused by the RPP. Eq. (13) is also similar to the Wigner-filter and applied to remove the RPP modulation. In addition, β in this equation is a constant used to prevent divide-by-zero effect.

$$p'''_n(x, y) = p''_n(x, y) + \frac{\left|t(x, y)\right|}{\left|t(x, y)\right|_{\max}} \frac{t(x, y)^*}{\left(\left|t(x, y)\right|^2 + \beta\right)} \cdot [\psi'''_n(x, y) - \psi''_n(x, y)] \tag{13}$$

17) Back propagate $p'''_n(x, y)$ to the object plane to calculate the updated exiting wave of object $u'''_n(x, y)$ as $u'''_n(x, y) = \Im_{d_1}^{-1}\{p'''_n(x, y)\}$.
18) Update the exiting wave of object on the object plane and it is used as the initial guess in the $(n+1)$th iteration as $u_{n+1}(x, y)$:

$$u_{n+1}(x, y) = [u'''_n(x, y) + u''_n(x, y)]/2 \cdot S(x, y) \tag{14}$$

19) Repeat procedures (2) to (18) until the reconstructed image satisfies the required accuracy.

With the above iterative computation, the undesired twin image and the zero-order diffraction in on-axis DH can be effectively removed and a high-quality reconstructed image can be obtained. It is worth noting that with modulated diffraction pattern and pre-measured RPP distribution in Fig. 2(b), the object information can also be reconstructed with coherent modulation imaging (CMI) [24]–[27]. However, the resolution of reconstructed image in CMI is still lower than expected as is influenced by speckle noise in practice.

According to this method, the hologram and the modulated diffraction pattern should be recorded; moreover, the RPP feature as well as d_2 should be precisely measured before sample detection. All these details are illustrated in the following section.

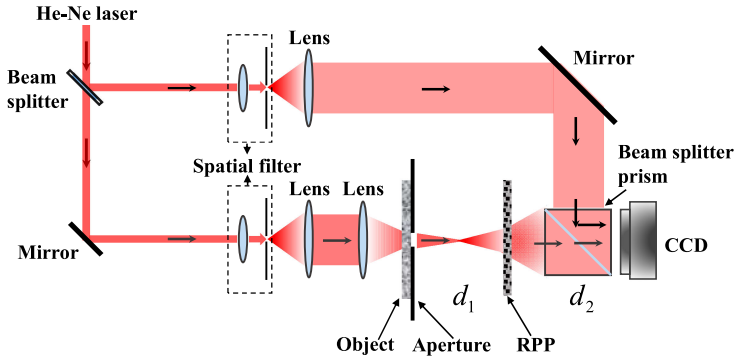

Fig. 3. The experimental setup. The focal length of the lens is 125 mm, and the beam splitter prism used is 25.4 mm in width. d1 is the distance between the aperture and the RPP; d2 is the distance between the RPP and the CCD.

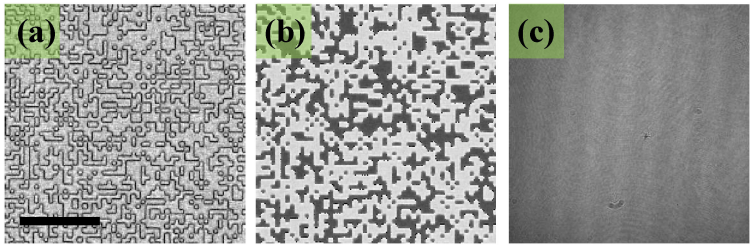

Fig. 4. Premeasured distributions. (a) and (b) are the modulus and phase distribution of the RPP measured through the PIE experiment. (c) The distribution of the reference wave. The scale bar in (a) is 600 μm.

3. Experimental Verification

Fig. 3 reveals the optical system of the proposed method. A laser beam with the wavelength of 632.8 nm was divided into two beams using a beam splitter, one serves as the reference wave after passing through a spatial filter and a collimating lens, while another forms a modulated diffraction pattern after illuminating on the object and modulated by the RPP. Though both dispersed and converging illumination beams can be used in this method, in order to expand the FOV of the object, a converging beam was preferred as shown in Fig. 3. The on-axis hologram and the modulated diffraction pattern were recorded by a CCD camera (Pike F1100b, Allied Vision) with cropped pixels of 2000 $\times$ 2000 and pixel size of 9 $\times$ 9 μm^2. The aperture used to restrict the object was 2 mm in diameter. Moreover, d_1 and d_2 were measured as 128.6 mm and 92.4 mm, respectively.

In experiments, the distribution of RPP and reference wave were measured in advance. The RPP used in experiments was manufactured by photolithography with phase difference of 0 and π, which is randomly distributed with the illumination wavelength of 632.8 nm with pixel size of 18 $\times$ 18 μm^2, and was accurately measured through Ptychographic Iterative Engine (PIE) [28]–[30]. The experimental setup shown in Fig. 3 can be used as a PIE setup to recording a series of diffraction patterns of RPP during its 2D scanning but by blocking the reference light and removing the object. Moreover, due to the prism, d_2 as the actual distance between the RPP and the CCD camera can hardly be measured with conventional measuring devices, while can be precisely determined by PIE method [28]–[30]. With accurately measured d_2, both the RPP modulus and phase distribution at its position can be measured in extremely high accuracy as shown in Fig. 4(a) and Fig. 4(b), respectively, as well as d_2, which can support high accurate phase retrieval of the proposed method. Besides, in on-axis DH, the distribution of reference wave can be measured as the square root of the recorded intensity of reference wave and is shown in Fig. 4(c). Both the

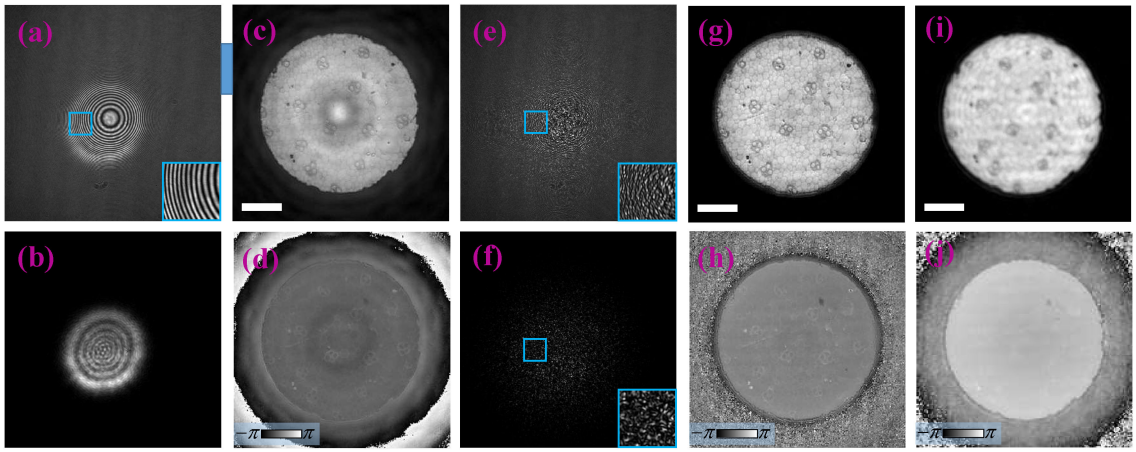

Fig. 5. Experimental results. (a) and (b) are hologram and diffraction pattern recorded in ordinary on-axis DH; (c) and (d) are reconstructed modulus and phase in ordinary on-axis DH. (e) and (f) are hologram and modulated diffraction pattern recorded in suggested on-axis DH; (g) and (h) are reconstructed modulus and phase in suggested DH; (i) and (j) are reconstructed modulus and phase with CMI method. The scale bar is 500 μm in (c), (g) and (i). Images in the color solid box are zoomed for observation.

measured distribution of the RPP and reference wave were kept unchanged if the illumination in experiments remain stable.

A stem of monocotyledon T.S was first used as the object to demonstrate the feasibility of the suggested method. To evaluate its effectiveness, a group of ordinary holographic data by removing the RPP and a group of the suggested holographic data with the RPP were captured as shown in Fig. 5. Where Fig. 5(a) and Fig. 5(b) show the hologram and diffraction pattern recorded in ordinary on-axis DH, respectively. Fig. 5(c) and Fig. 5(d) show the reconstructed modulus and phase image with traditional spatial filtering backpropagation method [20] by subtracting the zero-order information, most of the zero-order diffraction information was removed and the contour structure of the object was reconstructed, while the residual information of undesired twin image and zero-order diffraction still occurred thus resulting in a poor-quality reconstruction result. Fig. 5(e) and Fig. 5(f) show the hologram and modulated diffraction pattern obtained with the suggested on-axis DH method, and the reconstructed modulus and phase image using the suggested iterative algorithm with 100 iterations are shown in Fig. 5(g) and Fig. 5(h), respectively. The structure of the reconstructed object was clear and the undesired twin image and zero-order diffraction was removed effectively, proving the feasibility of the proposed method. Besides, the reconstruction results with CMI method by using the modulated diffraction pattern of Fig. 5(f) are presented in Fig. 5(i) and Fig. 5(j), both the modulus and phase information were reconstructed while the resolution of reconstructed image was lower than expected due to the speckle noise.

Another experiment was also implemented to image a standard USAF resolution target. Fig. 6(a) and Fig. 6(b) show the hologram and diffraction pattern recorded in ordinary on-axis DH, and the reconstruction results are shown in Fig. 6(c) and Fig. 6(d), respectively. Though the resolution in Fig. 6(c) reached about 12.4 μm (40.32 LP/mm) as shown in the zoomed-in image, the image quality was still poor with residual information of undesired twin image and zero-order diffraction overlapped. While using the suggested method dealing with recorded hologram and modulated diffraction pattern shown in Fig. 6(e) and Fig. 6(f), an improved reconstruction results were obtained with modulus and phase image shown in Fig. 6(g) and Fig. 6(h), respectively. Though the resolution in Fig. 6(g) shows no obvious increase as compared to Fig. 6(c), the image quality improved obviously while the undesired twin image and zero-order diffraction were removed effectively. The reconstruction results with CMI method are also presented, Fig. 6(i) and Fig. 6(j) show the modulus and phase information reconstructed from the modulated diffraction pattern of Fig. 6(f).

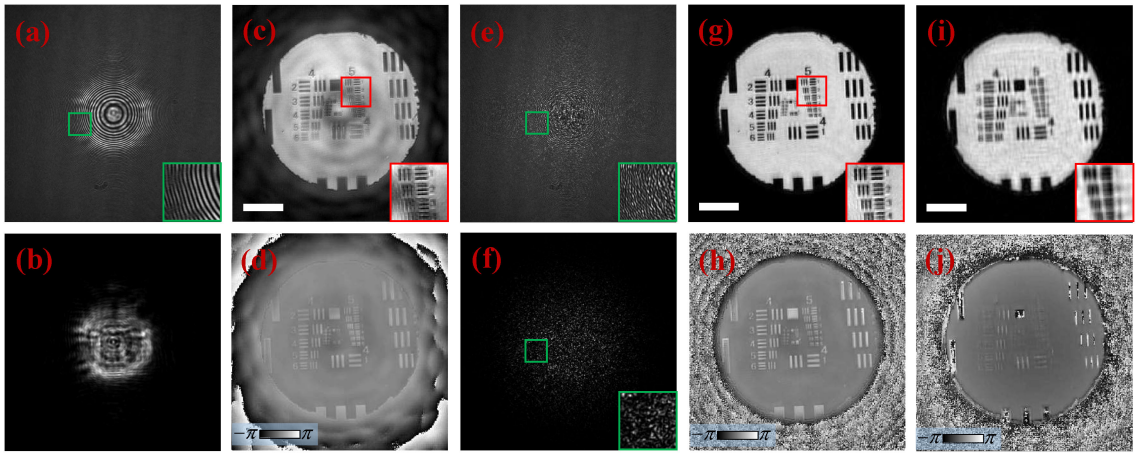

Fig. 6. Experimental results. (a) and (b) are hologram and diffraction pattern recorded in ordinary on-axis DH; (c) and (d) are reconstructed modulus and phase in ordinary on-axis DH. (e) and (f) are hologram and modulated diffraction pattern recorded in suggested on-axis DH; (g) and (h) are reconstructed modulus and phase in suggested DH; (i) and (j) are reconstructed modulus and phase with CMI method. The scale bar is 500 μm in (c), (g) and (i). Images in the color solid box are zoomed for observation.

The resolution in Fig. 6(i) reached about 22.1 μm (22.63 LP/mm), which is lower than Fig. 6(c) and Fig. 6(g). The experimental result is consistent with the former experiments, thus well proving the capability of our suggested method.

4. Discussion

4.1 Influence of the RPP Pixel Size on Reconstruction Performance

A key optical element used in the suggested method is the RPP, and the influence of the RPP pixel size on the performance of the suggested iterative algorithm is evaluated using numerical simulation. The assumed modulus and phase distributions of the object are shown in Fig. 7(a). The red dashed circles indicate the aperture with a diameter of 2 mm, which is used as the spatial constraint in the iterative computation. A collimated laser beam with the wavelength of 632.8 nm is used as the illumination, and the CCD camera is assumed to be 2000 $\times$ 2000 pixels with pixel size of 9 $\times$ 9 μm^2. The distance between the object and the RPP is 75 mm and the distance between the RPP and the CCD camera is 50 mm. The RPP with the phase difference of 0 and π has a structure shown in the inserted image of Fig. 7(b), which is randomly distributed with the illumination wavelength of 632.8 nm. Besides, Fig. 7(b) shows the modulated diffraction pattern and corresponding hologram recorded in on-axis DH with the RPP pixel size of 18 $\times$ 18 μm^2, the zoomed area in red solid boxes clearly show the difference between a diffraction pattern and a hologram.

In simulation, the reconstruction results are obtained using 50 iterations. Fig. 7(d) to Fig. 7(h) show the reconstruction results using 5 different RPPs with pixel sizes of 72 $\times$ 72 μm^2, 36 $\times$ 36 μm^2, 18 $\times$ 18 μm^2, 9 $\times$ 9 μm^2 and 4.5 $\times$ 4.5 μm^2, respectively. The result shows that the image quality of reconstructed modulus and phase images is inversely proportional to the RPP pixel size. Furthermore, to quantitatively evaluate the reconstruction accuracy, Eq. (15) is adopted to calculate the reconstruction error,

$$E_n = \frac{\sum_n \left| u(x, y) - u_n(x, y) \right|^2}{\sum \left| u(x, y) \right|^2} \tag{15}$$

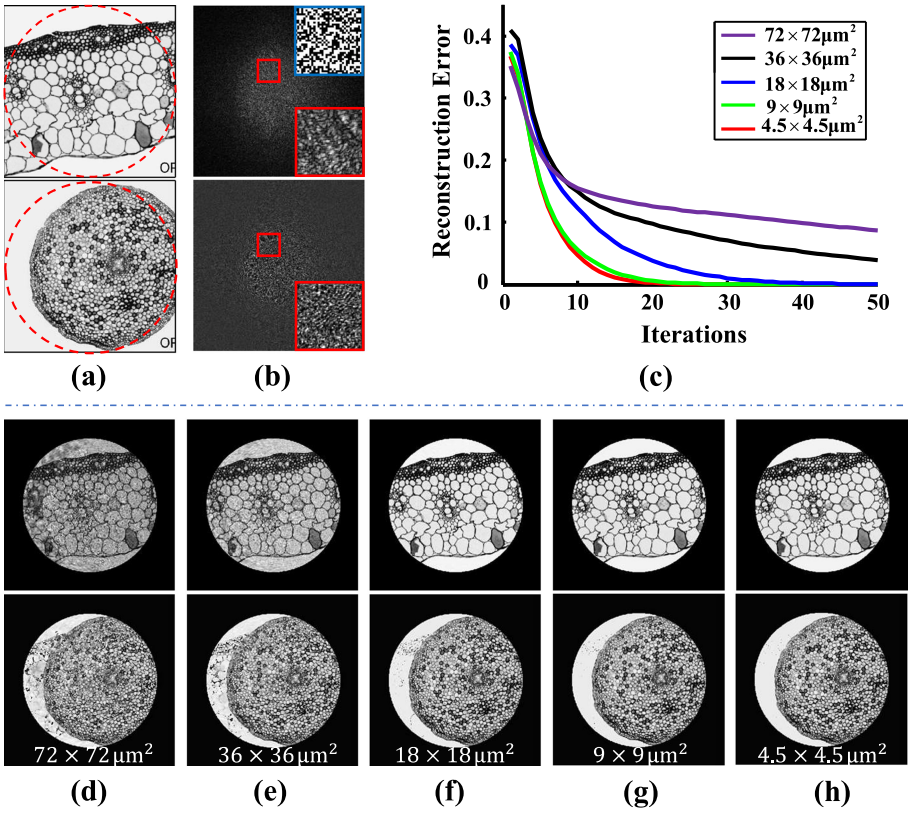

Fig. 7. (a) is assumed modulus and phase images of the object. (b) The modulated diffraction pattern and the corresponding hologram in on-axis DH. (c) The evaluation of the reconstruction errors change with the number of iterations. (d) to (h) are reconstructed modulus and phase with five RPPs of different pixel size of 72 × 72 μm^2, 36 × 36 μm^2, 18 × 18 μm^2, 9 × 9 μm^2 and 4.5 × 4.5 μm^2, respectively.

where $u_n(x, y)$ is the reconstructed object distribution after n iterations with the suggested method and $u(x, y)$ is the original object distribution. The reconstruction errors are shown in Fig. 7(c), where a small pixel size of 4.5 × 4.5 μm^2 shows a faster convergence and a lower reconstruction error, thus leading to a higher quality image in the reconstruction.

Though the simulation results show that a smaller pixel size of the RPP has a faster convergence and a lower reconstruction error. While in experiments, the RPP selection should be further considered. A smaller pixel size of the RPP can diffract more object information to the CCD camera. However, due to large angle scattering and the limited CCD camera size, the object information may not be completely collected. Additionally, the RPP with smaller pixel size can hardly be fabricated cost-effectively and measured accurately. Therefore, the RPP with pixel size of 18 × 18 μm^2 was chosen considering the balance which is cost-effective in fabrication but still guarantees high-quality in image reconstruction as shown in Fig. 7(c). From the above considerations, the RPP with pixel size of 18 × 18 μm^2 was chosen in experiments.

4.2 Comparisons to Other Methods

To further verify the feasibility of the suggested method in on-axis DH, a comparison was provided between the classical four-step phase shifting method [10] and the suggested method, and the numerical simulation results are shown in Fig. 8. Fig. 8(a) to Fig. 8(d) show four holograms generated with phase shifting, where the reference wave was varied with phase interval of π/2. The

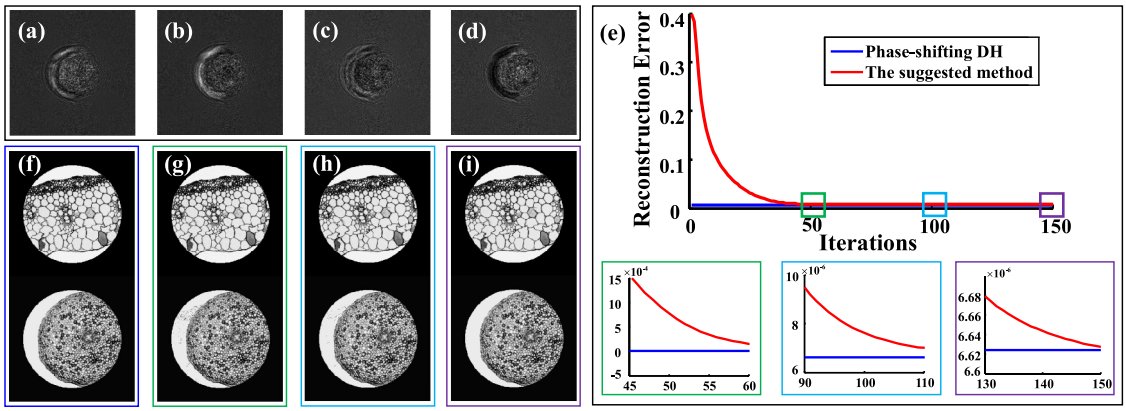

Fig. 8. (a) to (d) are hologram images generated with phase-shifting method. (e) The evaluation of the reconstruction error changes with the number of iterations. The solid box area are zoomed in to show the reconstruction accuracy between four step phase-shifting method and the suggested method. (f) The reconstruction result using the four step phase-shifting method. (g) to (i) are reconstruction results using the suggested method with 50 iterations, 100 iterations and 150 iterations, respectively.

reconstruction result is shown in Fig. 8(f), where high-quality images of modulus and phase can be retrieved. For comparison, Fig. 8(g) to Fig. 8(i) show the reconstruction results with the suggested method with 50 iterations, 100 iterations and 150 iterations, respectively. These reconstruction error is shown in Fig. 8(e). Both the modulus and phase distributions were effectively retrieved and the cross-talk information in phase image was removed with increase of iterations. Besides, with 150 iterations shown in Fig. 8(e), the reconstruction error with our suggested method could reach the same accuracy level as that of classical four step phase-shifting method, supporting that our suggested method can reconstruct a high-quality image in on-axis DH.

Another comparison between the classical iterative method [19] and the suggested method was also provided. Compared to the iterative method proposed in [19] (labelled as two-plane iteration method) which uses only two planes, the suggested method is a little complicated in data analysis since three planes are used. While the suggested method shows fast rate in convergence: a high-quality image can be reconstructed with 50 iterations even with complex-structured object, while only the simple-structured object can be reconstructed with the two-plane iteration method. The simulation results are shown below. Fig. 9 shows the simulation results using the two-plane iteration method and the suggested method, a simple structure as a narrow slit is used as the object shown in Fig. 9(a). Fig. 9(b) is the on-axis hologram, Fig. 9(c) and Fig. 9(d) are the modulated diffraction pattern and corresponding hologram, respectively. The reconstruction results with these two iteration methods are shown in Fig. 9(e) and Fig. 9(f). Besides, the reconstruction errors are quantitatively evaluated and shown in Fig. 9(g), where a high-quality image can be reconstructed with both methods.

While for reconstructing a complex-structured object with modulus and phase image shown in Fig. 10(a) and Fig. 10(b), these two methods show quite different results. Fig. 10(c) is the on-axis hologram with object constrained by an aperture, Fig. 10(d) and Fig. 10(e) are the modulated diffraction pattern and corresponding on-axis hologram, respectively. The reconstruction results using the two-plane iteration method are shown in Fig. 10(f) and Fig. 10(g), where the cross-talk information obviously appeared with 50 iterations. While using our suggested method, the reconstruction results are shown in Fig. 10(h) and Fig. 10(i), where most of cross-talk information was removed and high-quality images were reconstructed. Besides, the reconstruction errors shown in Fig. 10(j) clearly show the difference between these two methods, which well proves that the suggested method has a fast rate in convergence and can be used to reconstruct a complex-structured object with 50 iterations.

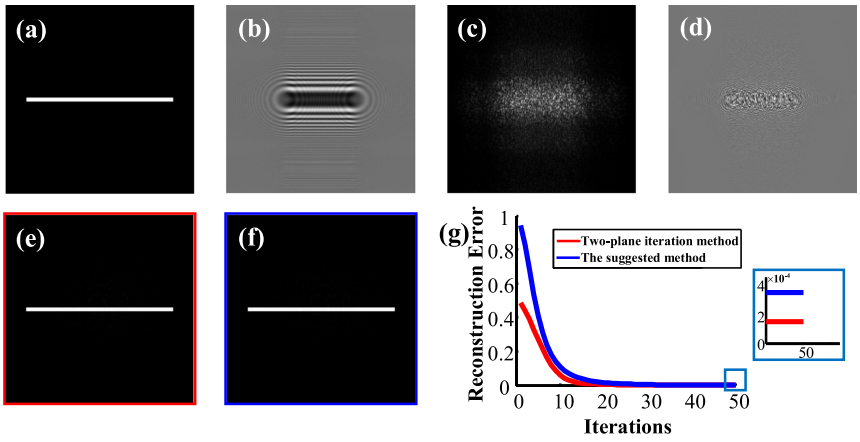

Fig. 9. (a) Simple-structured object as a narrow slit. (b) On-axis hologram used in two-plane iteration method. (c) and (d) Modulated diffraction pattern and the corresponding hologram in on-axis DH. (e) Reconstruction result using the two-plane iteration method. (f) Reconstruction result using the suggested method. (g) The evaluation of the reconstruction errors corresponding to the number of iterations.

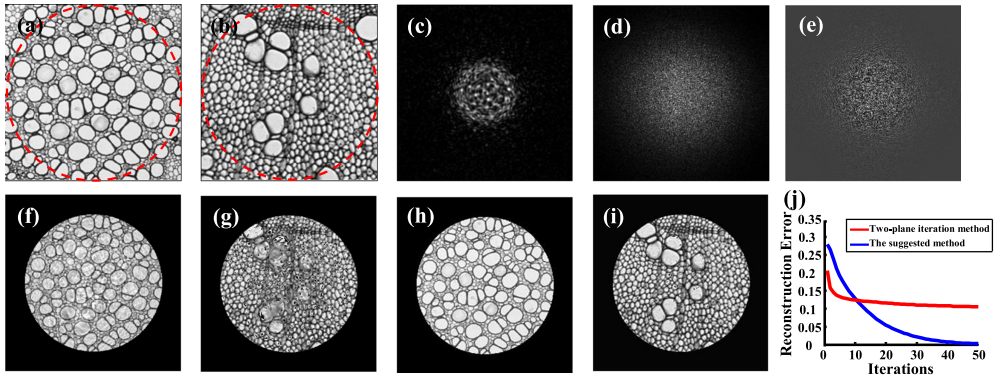

Fig. 10. (a) and (b) Modulus and phase of the complex-structured object. (c) On-axis hologram used in two-plane iteration method. (d) and (e) Modulated diffraction pattern and the corresponding hologram in on-axis DH. (f) and (g) Reconstruction results using the two-plane iteration method. (h) and (i) Reconstruction results using the suggested method. (j) The evaluation of the reconstruction errors corresponding to the number of iterations.

In our suggested method, an RPP is applied to modulate object and generate a modulated diffraction pattern. In addition, an RPP can also be used to modulate the reference wave to realize single-exposure phase-shifting DH [31]. In this method, a random-phase reference wave and diffraction pattern of the object are used to form the digital hologram. When the complex distribution of the reference wave is known in advance, the complex amplitude of the object can be obtained with single hologram. The computation algorithm assumes that the amplitude of the reference wave has the same value on each four adjacent pixels, while the phase distribution has different values. However, this assumption can be hardly realized since the amplitude of the reference wave is randomly distributed with modulation of the RPP, thus the results are often in poor quality with noise overlaid. While in our suggested method, no assumption is made and the noise is suppressed with the suggested iterative algorithm, thus providing a solution to reconstruct a high-quality image in on-axis DH. To verify the noise suppression capability of the suggested

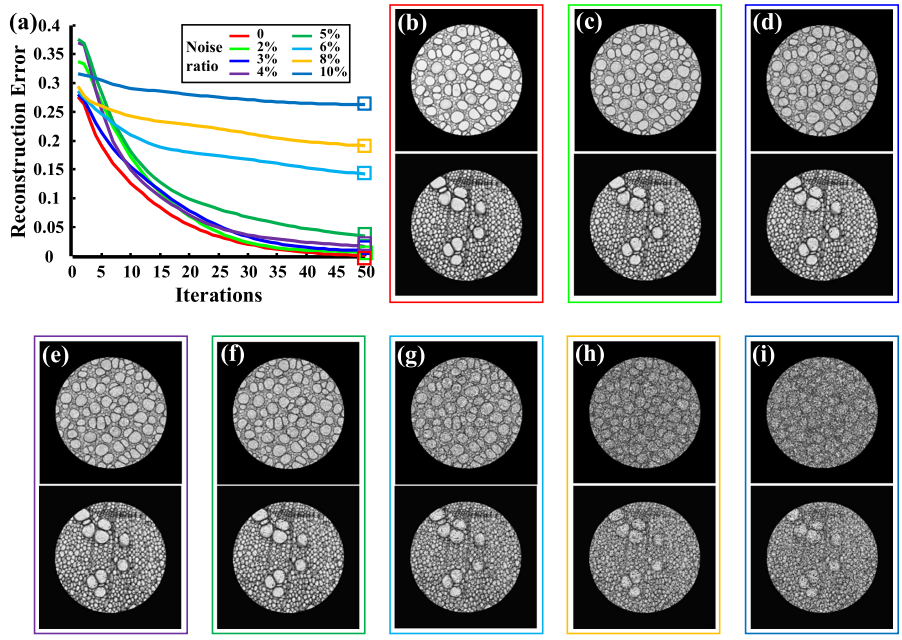

Fig. 11. (a) The reconstruction errors using the suggested method with 50 iterations at different noise level. (b) to (j) are reconstruction results at 50 iteration with random noise ratio of 0, 2%, 3%, 4%, 5%, 6%, 8%, 10%, respectively.

method, simulations were provided by adding different ratio of random noise to the holograms. Fig. 11 show the reconstruction errors and reconstruction results using the suggested method with 50 iterations at different noise level, where a moderate-quality image can also be reconstructed at high noise level (with random noise ratio of 5%) and support that the suggested method can be applied in a moderate noise environment.

5. Conclusion

In conclusion, we have demonstrated a phase retrieval method to reconstruct high-quality image free from undesired terms in on-axis DH with MCDI. An RPP is applied to modulate the object information and forms an on-axis digital hologram with a plane reference wave, then the corresponding iterative algorithm is designed to reconstruct the object information from the modulated diffraction pattern and corresponding on-axis digital hologram. The feasibility of the suggested on-axis DH method is verified with visible light experiments and numerical simulations. Though the resolution shows no obvious improvement in the suggested method as compared to ordinary on-axis DH, the image quality has significantly improved and the undesired twin image and zero-order diffraction have been effectively removed. Therefore, the proposed method can be a potential tool used in conditions requiring wave-front imaging in high resolution.

Acknowledgment

The authors wish to thank the anonymous reviewers for their valuable suggestions.

References

[1] L. Xu, X. Peng, J. Miao, and A. K. Asundi, “Studies of digital microscopic holography with applications to microstructure testing,” *Appl. Opt.*, vol. 40, no. 28, pp. 5046–5051, 2001.

[2] P. Ferraro *et al.*, "Extended focused image in microscopy by digital holography," *Opt. Express*, vol. 13, no. 18, pp. 6738–6749, 2005.
[3] F. Dubois, N. Callens, C. Yourassowsky, M. Hoyos, P. Kurowski, and O. Monnom, "Digital holographic microscopy with reduced spatial coherence for three-dimensional particle flow analysis," *Appl. Opt.*, vol. 45, no. 5, pp. 864–871, 2006.
[4] S. Li and Y. Zhao, "SNR enhancement in in-line particle holography with the aid of off-axis illumination," *Opt. Express*, vol. 27, no. 2, pp. 1569–1577, 2019.
[5] S. Vasudevan, G. C. Chen, Z. Lin, and B. K. Ng, "Quantitative photothermal phase imaging of red blood cells using digital holographic photothermal microscope," *Appl. Opt.*, vol. 54, no. 14, pp. 4478–4484, 2015.
[6] V. P. Pandiyan and R. John, "Optofluidic bioimaging platform for quantitative phase imaging of lab on a chip devices using digital holographic microscopy," *Appl. Opt.*, vol. 55, no. 3, pp. A54–A59, 2016.
[7] C. Yuan, H. Zhai, X. Wang, and L. Wu, "Lensless digital holography with short-coherence light source for three-dimensional surface contouring of reflecting micro-object," *Opt. Commun.*, vol. 270, no. 2, pp. 176–179, 2007.
[8] P. T. Samsheerali, K. Khare, and J. Joseph, "Three-dimensional display system using near on-axis, phase-only digital holography," *Appl. Opt.*, vol. 54, no. 3, pp. 451–457, 2015.
[9] E. Cuche, P. Marquet, and C. Depeursinge, "Spatial filtering for zero order and two image elimination in digital off axis holography," *Appl. Opt.*, vol. 39, no. 23, pp. 4070–4075, 2000.
[10] I. Yamaguchi and T. Zhang, "Phase-shifting digital holography," *Opt. Lett.*, vol. 22, no. 16, pp. 1268–1270, 1997.
[11] G. Pedrini, W. Osten, and Y. Zhang, "Wave-front reconstruction from a sequence of interferograms recorded at different planes," *Opt. Lett.*, vol. 30, no. 8, pp. 833–835, 2005.
[12] Y. Awatsuji, M. Sasada, and T. Kubota, "Parallel quasi-phase-shifting digital holography," *Appl. Phys. Lett.*, vol. 85, no. 6, pp. 1069–1071, 2004.
[13] Y. Awatsuji *et al.*, "Parallel two-step phase-shifting digital holography," *Appl. Opt.*, vol. 47, no. 19, pp. D183–D189, 2008.
[14] T. Tahara *et al.*, "Parallel two-step phase-shifting digital holography using polarization," *Opt. Rev.*, vol. 17, no. 3, pp. 108–113, 2010.
[15] P. Gao *et al.*, "Parallel two-step phase-shifting digital holograph microscopy based on a grating pair," *J. Opt. Soc. Amer. A*, vol. 28, no. 3, pp. 434–440, 2011.
[16] C. Tian and S. Liu, "Phase retrieval in two-shot phase-shifting interferometry based on phase shift estimation in a local mask," *Opt. Express*, vol. 25, no. 18, pp. 21673–21683, 2017.
[17] T. D. Yang, H. J. Kim, K. J. Lee, B. Kim, and Y. Choi, "Single-shot and phase-shifting digital holographic microscopy using a 2-D grating," *Opt. Express*, vol. 24, no. 9, pp. 9480–9488, 2016.
[18] H. Zhang, T. Stangner, K. Wiklund, and M. Andersson, "Object plane detection and phase retrieval from single-shot holograms using multi-wavelength in-line holography," *Appl. Opt.*, vol. 57, no. 33, pp. 9855–9862, 2018.
[19] T. Latychevskaia and H. Fink, "Solution to the twin image problem in holography," *Phys. Rev. Lett.*, vol. 98, no. 23, 2007, Art no 233901.
[20] T. Latychevskaia, "Iterative phase retrieval for digital holography: Tutorial," *J. Opt. Soc. Amer. A*, vol. 36, no. 12, pp. D31–D40, 2019.
[21] F. Li, W. Yan, P. Tian, F. Yang, and F. Peng, "Twin image reduction method for digital in-line holography by using a digital periphery," *Optik*, vol. 193, 2019, Art. no. 162988.
[22] W. Zhang *et al.*, "Twin-Image-Free holography: A compressive sensing approach," *Phys. Rev. Lett.*, vol. 121, no. 9, 2018, Art. no. 093902.
[23] Z. Jiang, S. P. Veetil, J. Cheng, C. Liu, L. Wang, and J. Zhu, "High-resolution digital holography with the aid of coherent diffraction imaging," *Opt. Express*, vol. 23, no. 16, pp. 20916–20925, 2015.
[24] F. Zhang and J. M. Rodenburg, "Phase retrieval based on wave-front relay and modulation," *Phys. Rev. B*, vol. 82, no. 12, 2010, Art. no. 121104.
[25] F. Zhang, B. Chen, G. R. Morrison, J. Vilacomamala, M. Guizarsicairos, and I. K. Robinson, "Phase retrieval by coherent modulation imaging," *Nat. Commun.*, vol. 7, no. 1, 2016, Art. no. 121104.
[26] H. Tao, S. P. Veetil, X. Pan, C. Liu, and J. Zhu, "Lens-free coherent modulation imaging with collimated illumination," *Chin. Opt. Lett.*, vol. 14, no. 7, 2016, Art. no. 071203.
[27] X. Dong, X. Pan, C. Liu, and J. Zhu, "Single shot multi-wavelength phase retrieval with coherent modulation imaging," *Opt. Lett.*, vol. 43, no. 8, pp. 1762–1765, 2018.
[28] H. M. L. Faulkner and J. M. Rodenburg, "Movable aperture lensless transmission microscopy: A novel phase retrieval algorithm," *Phys. Rev. Lett.*, vol. 93, no. 2, 2004, Art. no. 023903.
[29] A. M. Maiden and J. M. Rodenburg, "An improved ptychographical phase retrieval algorithm for diffractive imaging," *Ultramicroscopy*, vol. 109, no. 10, pp. 1256–1262, 2009.
[30] F. Zhang *et al.*, "Translation position determination in ptychographic coherent diffraction imaging," *Opt. Express*, vol. 21, no. 11, pp. 13592–13606, 2013.
[31] T. Nomura and M. Imbe, "Single-exposure phase-shifting digital holography using a random-phase reference wave," *Opt. Lett.*, vol. 35, no. 13, pp. 2281–2283, 2010.